

## Oxygen Annealing of Ex-Situ YBCO/Ag Thin-Film Interfaces

J. W. Ekin, C. C. Clickner, S. E. Russek, and S. C. Sanders

Electromagnetic Technology Division, National Institute of Standards and Technology, Boulder, CO USA

**Abstract**— The resistivity of YBCO/Ag interfaces has been measured for different oxygen annealing temperatures for a series of ex-situ fabricated thin-film contacts having sizes ranging from  $16\ \mu\text{m} \times 16\ \mu\text{m}$  down to  $4\ \mu\text{m} \times 4\ \mu\text{m}$ . The interface resistivity began to decrease after annealing at  $300^\circ\text{C}$  for 10 minutes in one atmosphere oxygen. After annealing at  $400^\circ\text{C}$ , the contact resistivity decreased by several orders of magnitude to the  $10^{-7}\ \Omega\text{-cm}^2$  range. The 500-nm thick Ag layer showed massive surface diffusion and agglomeration for annealing temperatures above  $400^\circ\text{C}$ ; this temperature thus represents a practical limit for oxygen annealing the YBCO/Ag interface system for more than 10 minutes. Rapid cooling of the chip after annealing led to a severe loss of critical current density in the YBCO layer, which could be restored by reannealing and cooling at a slower rate of  $50^\circ\text{C}/\text{min}$ . The relative shape of the conductance-vs.-voltage characteristics of the YBCO/Ag interface were essentially unaltered by oxygen annealing; the overall parabolic shape, superconducting gap features, and magnetic-scattering zero bias anomaly remained constant, even though the contact conductance increased by several orders of magnitude. These data suggest that the main reduction in interface resistivity arises from an enhancement of the effective contact area, not from a change in interface conduction mechanism.

### I. INTRODUCTION

An understanding of the interface properties of  $\text{YBa}_2\text{Cu}_3\text{O}_{7-\delta}$  (YBCO) is essential for fabricating reproducible device interfaces and forming reliable, practical contacts to this material. In this paper we report preliminary results on the effect of annealing temperature on thin-film YBCO/Ag contact interfaces. These contact interfaces were fabricated ex-situ; that is, the Ag counter electrode was deposited on the YBCO after the YBCO film had been removed from the deposition chamber and subjected to external surface contamination, including air exposure and lithographic processing. We focus here, in particular, on the following questions: (1) the temperature limits for silver balling up in practical planar contact geometries,

Manuscript received October 18, 1994.

Publication of NIST, not subject to copyright.

This work was supported in part by the Advanced Research Projects Agency under contract 7975. We wish to thank Conductus for YBCO film samples used in an accompanying test.

(2) the improvement of contact resistivity to be expected for ex-situ thin-film YBCO/Ag contacts from oxygen annealing, and (3) the effect of oxygen annealing on the tunneling characteristics and zero-bias anomaly that is seen in unannealed YBCO/noble metal interfaces.<sup>1,2,3,4</sup>

### II. SAMPLE AND MEASUREMENTS INFORMATION

YBCO films 200-nm thick were pulse-laser deposited on (100)  $\text{LaAlO}_3$  or (100)  $\text{MgO}$  substrates. The base pressure in the chamber at deposition temperature was about  $10^{-5}$  to  $10^{-4}$  Pa (about  $10^{-7}$  to  $10^{-6}$  Torr). After deposition, the YBCO films were slowly cooled to room temperature over a time period of about 45 minutes in an oxygen atmosphere of 26.7 kPa (200 Torr). The resulting YBCO films were c-axis oriented with a (005) rocking curve having a full width at half maximum of  $< 0.5^\circ$ ,  $T_c$  in the range 86-91 K, and  $J_c$ 's in the range  $1\text{-}2 \times 10^6\ \text{A}/\text{cm}^2$  at 77 K in zero magnetic field. AFM/STM studies indicate that the area of the YBCO a,b-edges was about 5% of the c-axis area.<sup>5</sup> The YBCO samples were then photolithographically patterned to define square planar contact interfaces with sides of 16, 8, 4, and 2  $\mu\text{m}$  using a test pattern designed to minimize sheet resistance contributions to the measured contact resistivity  $\rho_c$ . This was confirmed by the constancy of the measured  $\rho_c$  with contact area for the results reported here. The  $\text{MgO}$  layer that defines the contact size was deposited by magnetron sputtering. Finally, the 500 nm thick Ag counter electrodes were evaporatively deposited after lightly ion milling the YBCO surface at 200 V in an Ar-20%  $\text{O}_2$  gas mixture. Conductance curves were obtained by differentiating the current vs. voltage (I-V) data using a moving three-point fit.

The quality of the  $\text{MgO}$  insulation layer that defined the contact area was tested for each chip using three YBCO/Ag cross strips separated by  $\text{MgO}$ . In several of the chips, the  $\text{MgO}$  layer was less than 29 nm thick instead of the usual 42 nm. These chips failed the insulation test at higher annealing temperatures, presumably from silver diffusion through pinholes in the  $\text{MgO}$  insulation, which effectively shunted the contact testers. From the insulation tests we calculate that in these chips the resistance through the insulation layer  $R_{\text{insul}}$  was only 2 to 3 times that of the apparent contact resistance  $R_c$  after annealing at  $500^\circ\text{C}$ . Also, the contact resistivity  $\rho_c$  for these low  $R_{\text{insul}}$  chips became nearly ohmic at high annealing temperatures, and the  $\rho_c$  results did not scale with contact area. Here we report just

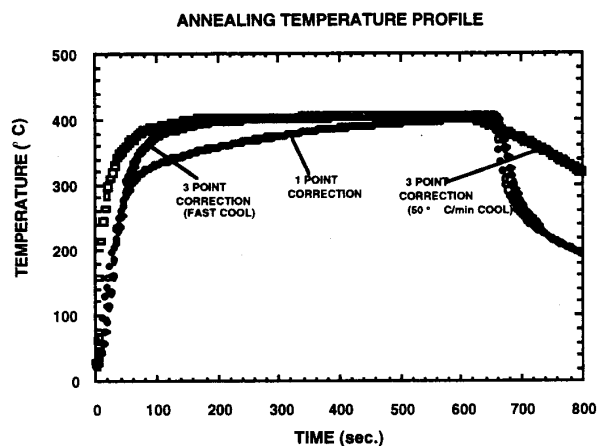


Fig. 1 Substrate-surface temperature vs. time for the rapid thermal annealer, showing one-point correction, three-point correction, and slow-cool characteristics. Rapidly cooling the YBCO/Ag interface after annealing resulted in a reduction of  $J_c$  in the YBCO layer by 79% and a broadening of the  $T_c$  transition, due to oxygen disorder. Reannealing in oxygen with a slower cooldown rate of 50°C/min restored both  $J_c$  and  $T_c$  to their original values.

the results for the chips with the thicker MgO layer, which passed the insulation test ( $R_{\text{insul}}/R_c > 100$ ).

### III. RAPID THERMAL ANNEALING APPARATUS AND PROCEDURE

Oxygen annealing of the contact test chips was carried out in one atmosphere of oxygen using a quartz-lamp rapid thermal annealing (RTA) apparatus. Temperature in the RTA was controlled by a feedback thermocouple attached to a small chip of Si. The apparatus was calibrated in a separate

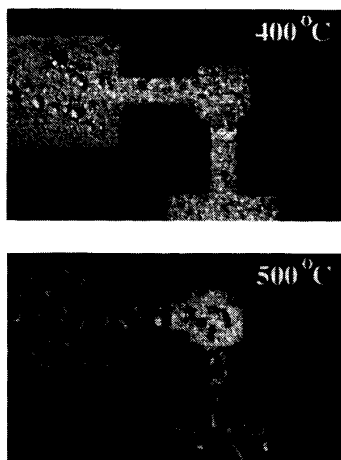


Fig. 2 Optical micrographs of the 8  $\mu\text{m}$  x 8  $\mu\text{m}$  contact tester as a function of anneal temperature. Above 400°C, extensive diffusion of Ag occurred, leading to Ag agglomeration and eventual loss of continuity through the Ag thin-film.

experiment using another thermocouple thermally anchored directly to the surface of a dummy test chip using silver paste. Initially, the RTA was calibrated by ramping the control thermocouple to a fixed temperature, but this resulted in the temperature of the contact test chip slowly increasing throughout the 10 minute anneal, as shown by the "one-point correction" curve in Fig. 1. The sloping temperature curve was then adjusted to be nearly flat using a three-setpoint scheme that corrected for the difference in thermal response time between the control thermocouple and the test chip. However, we then learned that the rapid cooldown of the contact test chip resulted in degradation of  $T_c$  and nearly a 79% loss in critical current density of the YBCO film. This we ascribe to oxygen disorder<sup>6</sup> because, on reannealing at the same temperature with a slower 50°C/min cooldown rate, the critical-current density was fully restored to its initial preannealed value.

### IV. RESULTS

#### A. Ag agglomeration problem

Figure 2 shows the contact surface after 400°C and 500°C anneals. The anneal times were 10 minutes with a relatively slow cooldown as shown in Fig. 1. Up to annealing temperatures of about 300°C to 350°C, the diffusion of Ag was limited enough that only growth in the size of Ag crystals is seen in the micrographs. After the 400°C anneal, however, considerable Ag crystal growth is seen, but the Ag film is still continuous. However, after the 500°C anneal, the Ag crystal growth is so extensive that the Ag ceases to wet the surface, coalescing into crystals that look like partially connected balls. This was particularly true where the Ag film coated the insulating substrate directly. The problem was less severe where the Ag film covered the YBCO film. Thus, 400°C represents a practical temperature limit for oxygen annealing these 500 nm thick Ag films. The temperature limit will be somewhat higher for thicker films.<sup>7</sup> An oxygen annealing temperature of 400°C, however, is adequate for nearly reaching the lower limit of contact resistivity that can be attained for these YBCO/Ag interfaces.

#### B. Effect of annealing on the temperature dependence of the YBCO/Ag interface resistivity

The temperature dependence of the contact resistivity  $\rho_c$  is shown in Fig. 3. As fabricated, these ex-situ contacts have a semiconducting character, with their interface resistivity rising as temperature is reduced. At about 90 K, the YBCO lines leading to the contact become superconducting and there is a decrease in the apparent contact resistivity as the sheet resistivity of the YBCO film becomes negligible. Semiconducting-like behavior continues until an annealing temperature of 400°C is reached. At this temperature there is an abrupt change. The high-temperature region becomes dominated by the metallic YBCO spreading resistance. The relative decrease in measured resistivity at 90 K is now

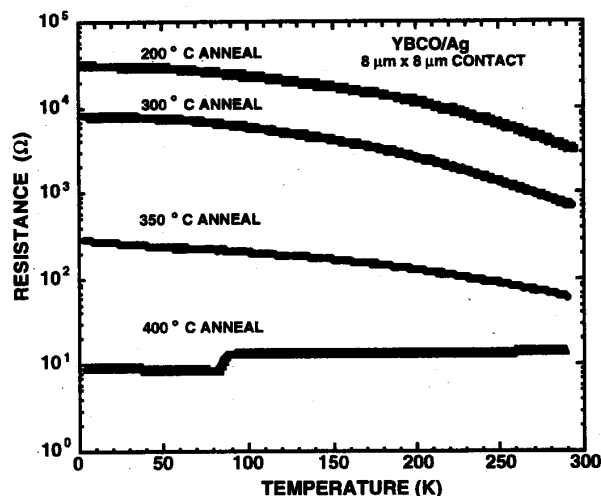


Fig. 3 Contact interface resistance vs. temperature for an ex-situ YBCO/Ag interface after annealing for 10 minutes in oxygen at different temperatures. The characteristic transforms abruptly from being semiconductor-like to metallic in nature after oxygen annealing at 400°C.

pronounced, and below  $T_C$  the contact resistivity is nearly constant with temperature.<sup>8</sup>

#### C. Effect of annealing on the magnitude of the YBCO/Ag resistivity below $T_C$

The value of the contact resistivity at 4 K (which is representative of the entire temperature range below  $T_C$  as shown in Fig. 3) is plotted for different contact devices on different chips in Fig. 4. For these chips, there was good agreement of the results among contacts of different size, indicating the absence of sheet resistivity effects in the Ag

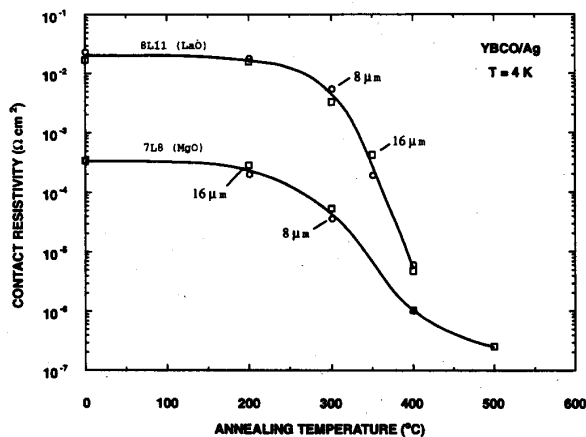


Fig. 4 Contact interface resistivity as a function of annealing temperature for two different chips having differently sized YBCO/Ag contact interfaces. Each chip was annealed for 10 minutes in oxygen at progressively higher temperature. The contact resistivity decreases by more than three orders of magnitude at annealing temperatures above 300°C. Above 400°C the Ag film sometimes lost electrical continuity from excessive Ag surface diffusion and agglomeration.

counter electrode. As annealing temperature is increased, the contact resistivity remains initially unchanged until an annealing temperature above 200 °C is reached. At 300 °C  $\rho_C$  starts to decrease precipitously and by 400 °C it has decreased several orders of magnitude from its initial unannealed value. The improvement reached a limit in the  $10^{-7} \Omega\text{-cm}^2$  range for these ex-situ contacts. Annealing at temperatures of 500°C destroys the electrical continuity of the Ag film leading to the contact.

#### D. Effect of annealing on the conductivity characteristic of the YBCO/Ag interface

Conductance across a typical YBCO/Ag interface is shown as a function of bias voltage in Fig. 5. Initially with no annealing, there is a slightly asymmetric, parabolically shaped conductance characteristic, indicative of tunneling

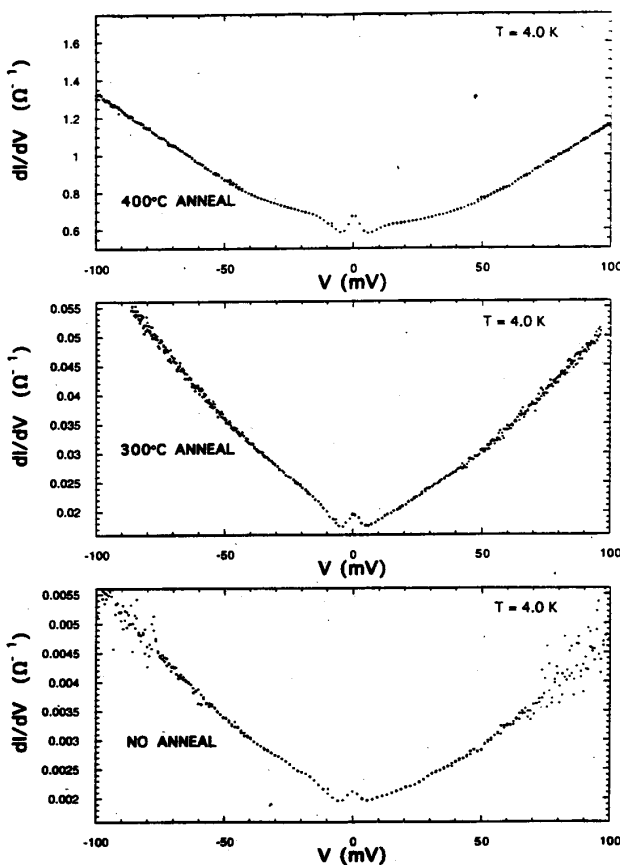


Fig. 5 Conductance vs. bias voltage for an  $8 \mu\text{m} \times 8 \mu\text{m}$  YBCO/Ag contact interface after oxygen annealing at different temperatures. The relative shape of the conductance characteristics, including the parabolic background, gap depression, and zero bias anomaly, are unchanged even though the interface conductance increased by several orders of magnitude.

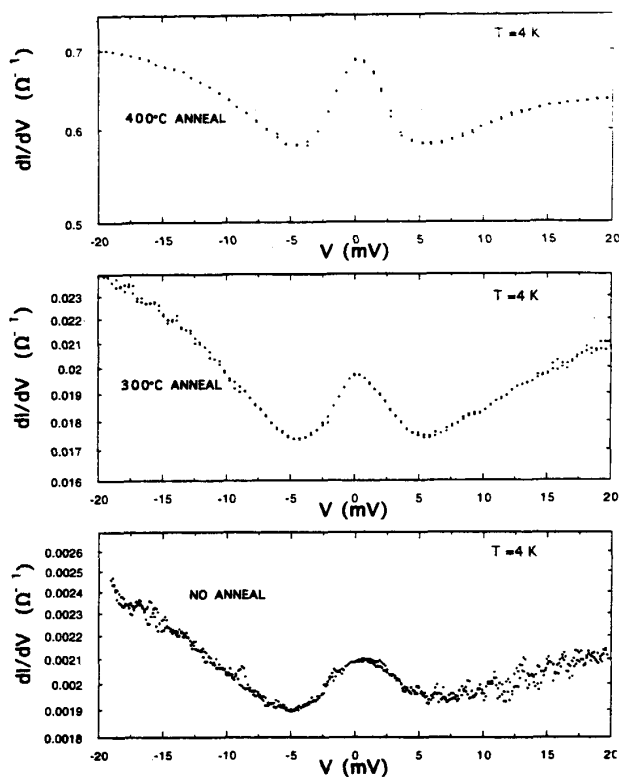


Fig. 6 Detail of the zero bias anomaly as a function of oxygen annealing temperature for the same YBCO/Ag interface as in Fig. 5. Each curve is plotted on a semilogarithmic graph with the same scaling factor, showing that the relative height of the zero bias anomaly does not change through the annealing process.

across the superconductor/normal metal (S/N) interface. The gap depression below about 20 mV can also be seen as well as a peak in conductance near zero bias. This zero bias anomaly has been identified as magnetically assisted tunneling across a barrier at the YBCO surface.<sup>1-4</sup> As seen in Fig. 6, the relative magnitude of the zero bias anomaly (ZBA) in these S/N junctions is about 10% of the conductivity of the interface, in good agreement the other S/N interface measurements covering a wide range of conductivity in the as-fabricated junctions.<sup>4</sup> The remarkable constancy of all these features through the annealing tests is shown by the graphs in Figs. 5 and 6. As the conductance of the contact changed by several orders of magnitude with increased anneal temperature, the relative shape of the curves remained essentially unchanged.

From earlier Auger depth-profile studies on bulk YBCO/Ag interfaces, we showed that the improvement of contact conductivity from annealing could be due to either diffusion of the noble metal through the interface barrier, or oxygen diffusion to replenish that lost at the surface of the YBCO.<sup>9</sup> Both processes were demonstrated, but it was

unclear which process dominated the improvement in  $\rho_c$  brought about by annealing. Recently we showed that the ZBA has the same relative character over a very wide range of YBCO junctions, regardless of reaction barrier thickness and whether the junction was fabricated in-situ or ex-situ; this indicates that the magnetic scatterers causing the ZBA occur at the surface of the YBCO layer, not in the interior of the reaction barrier.<sup>4</sup> The fact that the ZBA did not change in the present oxygen annealing tests leads us to believe that the magnetically assisted tunneling mechanism at the YBCO surface did not change. Rather the improvement in contact resistivity from annealing arises through a change in the effective contact area, either from diffusion of Ag along grain boundaries in the film, or an enhancement in the ratio of high- to low-conducting contact area at the interface.

## V. CONCLUSION

Improvements in the contact resistivity to the  $10^{-7} \Omega\text{-cm}^2$  range for YBCO/Ag contacts can be made for ex-situ fabricated contacts by annealing them in oxygen. This applies to contacts made in typical high-vacuum systems; further improvements may be possible for contacts made to YBCO surfaces cleaned in a better vacuum system. The best temperature for oxygen annealing the YBCO/Ag interface system is about 400°C for a 10 minute anneal, since at lower temperatures the improvement in contact resistivity is significantly less, and at higher temperatures massive silver diffusion starts to occur, accompanied by large crystal growth and loss of electrical continuity in the silver film. The constancy of the shape of the conductivity vs. bias voltage characteristic of these YBCO/Ag junctions over the entire range of annealing temperatures suggests that the main reduction in interface resistivity arises from an enhancement of the effective contact area, not from a change in interface conduction mechanism.

<sup>1</sup>J. Lesueur, L. H. Greene, W. L. Feldmann, and A. Inam, *Physica C* **191**, 325 (1992).

<sup>2</sup>T. Walsh, J. Moreland, R. H. Ono, and T. S. Kalkur, *Phys. Rev. Lett.* **66**, 516 (1991); T. Walsh, *Int. J. Mod. Phys. B* **6**, 125 (1992).

<sup>3</sup>A. M. Cucolo and R. Di Leo, *Phys. Rev. B* **47**, 2916 (1993).

<sup>4</sup>S. C. Sanders, S. E. Russek, C. C. Clickner, and J. W. Ekin, *Appl. Phys. Lett.* **65**, 2232 (1994).

<sup>5</sup>S. E. Russek, A. Roshko, S. C. Sanders, D. A. Rudman, J. W. Ekin, and J. Moreland, *Mat. Res. Soc. Symp. Proc.* **285**, 305 (1993).

<sup>6</sup>B. H. Moeckly, D. K. Lathrop, and R. A. Buhrman, *Phys. Rev. B* **47**, 400 (1993).

<sup>7</sup>A. Roshko, R. H. Ono, J. A. Beall, J. Moreland, A. J. Nelson, and S. E. Asher, *IEEE Trans. Mag.* **27**, 1616 (1991).

<sup>8</sup>J. W. Ekin, S. E. Russek, C. C. Clickner, and B. Jeanneret, *Appl. Phys. Lett.* **62**, 369 (1993)

<sup>9</sup>J. W. Ekin, T. M. Larson, N. F. Bergren, A. J. Nelson, A. B. Swartzlander, L. L. Kazmerski, A. J. Panson, and B. A. Blankenship, *Appl. Phys. Lett.* **52**, 1819 (1988).